Inorganica Chimica Acta, 203 (1993) 239–247

^{35}Cl nuclear quadrupole resonance and crystal structures of small guest molecules in tris(2,4-pentanedionate)M(III) inclusion compounds

L. Pang*, M. A. Whitehead
Department of Chemistry, McGill University, 801 Sherbrooke Street West, Montreal, Que., H3A 2K6 (Canada)

and E. A. C. Lucken
Département de Chimie Physique, Université de Genève, 30 quai E. Ansermet, 1211 Geneva (Switzerland)

(Received June 2, 1992; revised September 11, 1992)

Abstract

Tris(acetylacetonate)M(III) complexes, where M = Al, V, Cr, Mn, Fe, Co and Ga, form inclusion compounds with different solvent molecules. The compounds have a host/guest ratio of 1:2 for the small guest molecules $CHCl_3$ and CH_2Cl_2 and of 1:1 for the slightly bigger guest molecules *trans*-CHCl=CHCl, CH_2ClCH_2Cl and CCl_4. The ^{35}Cl nuclear quadrupole resonance spectra of these clathrates have been measured in the temperature range 4–200 K. The site symmetry, the existence of different crystal phases, the molecular disorder and molecular motions of the guest molecules in the host cavities, and the host–guest interactions, were evaluated from the NQR frequency measurements. The crystal structures of the $M(AcAc)_3$/*trans*-CHCl=CHCl compounds were measured at room temperature and confirm the NQR results.

Introduction

Tris(acetylacetonate)M(III), $M(AcAc)_3$, complexes are six-coordinate chelate compounds, were M is a trivalent ion of aluminum or a first-row transition metal [1]. The molecule has an octahedral conformation in which the six oxygen atoms form three acetylacetonates coordinated to the central metal atom. X-ray analyses have shown that these complexes can crystallize in different crystal classes to reflect different packing arrangements [2].

Aluminum(III), chromium(III) and iron(III) acetylacetonates were observed to form 1:2 molecular adducts with the chloroform solvent over thirty years ago [3]. However, the study of this kind of inclusion compound is rare in the literature, and their clathration behaviour is unknown. This paper reports the results for the ^{35}Cl nuclear quadrupole resonance (NQR) and crystal structures studies of the $M(AcAc)_3$ clathrates (M = Al, V, Cr, Mn, Fe, Co and Ga) with the guest molecules CH_2Cl_2, $CHCl_3$, CCl_4, *trans*-CHCl=CHCl and CH_2ClCH_2Cl, and gives information on (i) the guest molecule site symmetry, (ii) the existence of different crystal phases, (iii) the mobility and the disorder of the guest molecules in the host cavities, and (iv) the host–guest interaction.

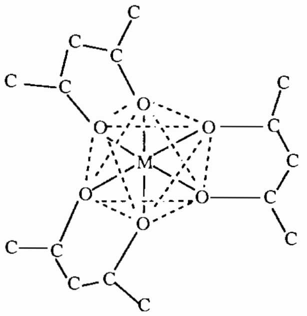

Experimental

Sample preparation

All the host molecules, which are commercially available (Johnson Matthey), were dissolved in the appropriate guest solvents. The crystals were formed on recrystallization and were stable as long as they were kept in the solvent atmosphere; they lose the guest molecules within half an hour when standing in air. The host/guest ratios of the clathrates were determined by using either ^{1}H NMR, weight loss analysis or, for compounds with known crystal structure, density mea-

---

*Author to whom correspondence should be addressed.

0020-1693/93/$6.00

surements. Freshly prepared crystalline samples for NQR spectroscopy were briefly dried and immediately sealed in glass vials. Single crystals of a suitable size of the corresponding clathrates for X-ray analyses were selected and removed from the mother liquor, quickly covered with epoxy to prevent deterioration and mounted on the tip of a glass fibre.

Nuclear quadrupole resonance

The NQR spectra from 4 to 200 K were measured on a Decca super-regenerative spectrometer and on a pulse spectrometer respectively, as described elsewhere [4].

The ^{35}Cl nuclear quadrupole resonance frequencies of *trans*-CHCl=CHCl, CH_2ClCH_2Cl, CCl_4, $CHCl_3$ and CH_2Cl_2 in different $M(AcAc)_3$ complexes are shown in Table 1.

Crystallographic measurement

Cell parameters and reflection intensities were measured at room temperature on a Rigaku diffractometer using graphite monochromated Mo Kα radiation. The accurate cell parameters were obtained by least-square analysis of at least 20 reflections in the range $25<2\theta<50°$. The crystal densities were measured by the suspension method using KI/H_2O solution. The crystal data of the $M(AcAc)_3$/*trans*-CHCl=CHCl (M=V, Cr, Mn, Fe, Co, Al and Ga) clathrates are listed in Table 2.

The structures of $Al(AcAc)_3$/*trans*-CHCl=CHCl and the $Ga(AcAc)_3$/*trans*-CHCl=CHCl were solved by direct methods, and the non-hydrogen atoms were refined anisotropically by least-squares analysis with the NRCVAX [5] programs. Atomic scattering factor and anomalous dispersion terms are taken from ref. 6. A

TABLE 1. ^{35}Cl nuclear quadrupole resonance frequencies

Guest	Host $M(AcAc)_3$	Host/guest ratio	ν_Q (MHz) 4 K	ν_Q (MHz) 77 K	$\lvert\Delta\nu_Q\rvert/\nu_Q^{iso}$ (%)
trans-CHCl=CHCl	Al	1:1		34.725	1.4
				35.273	
	Cr	1:1		34.724	1.5
				34.817	
				35.022	
				35.268	
	Mn	1:1		34.714	1.5
				35.244	
	Fe	1:1		34.722	1.4
				34.845	
				35.093	
				35.289	
	Co	1:1		34.692	1.6
				35.185	
	V	1:1	35.021	34.779	1.6
			35.386	35.073	
	Ga	1:1		34.723	1.4
				35.256	
CH_2ClCH_2Cl	Al	1:1		[a]	
	Cr	1:1	34.432	34.274	0.0
			34.669	34.432	
	Mn	1:1		33.998	0.1
				34.211	
				34.489	
				34.650	
	Fe	1:1	34.534	34.310	0.2
			35.851	34.561	
	Co	1:1		[a]	
$CHCl_3$	Al	1:2		37.172	2.5
				37.191	
				37.235	
				37.300	
				37.425	
				37.482	
				37.519	

(*continued*)

TABLE 1. (*continued*)

Guest	Host M(AcAc)$_3$	Host/guest ratio	ν_Q (MHz)		$\lvert\Delta\nu_Q\rvert/\nu_Q^{iso}$ (%)
			4 K	77 K	
	Cr	1:2		36.792	3.0
				36.987	
				37.195	
				37.535	
	Mn	1:2		37.223	2.3
				37.329	
				37.441	
				37.526	
	Co	1:2		36.785	2.3
				36.995	
				37.197	
				37.268	
				37.328	
				37.396	
				37.578	
				37.666	
				37.750	
				37.885	
CH_2Cl_2	Al	1:2		34.922	1.8
				35.169	
				35.222	
				35.464	
				35.574	
				35.657	
	Cr	1:2		34.633	1.9
				35.119	
				35.222	
				35.286	
				35.442	
				35.493	
				35.554	
				35.611	
	Fe	1:2		35.135	1.9
				35.173	
				35.379	
				35.511	
	Co	1:2		34.067	2.5
				34.240	
				34.712	
				34.772	
				34.992	
				35.162	
				35.179	
				35.213	
				35.303	
				35.335	
				35.442	
				35.506	
				35.624	
				35.648	
CCl_4	Al	1:1		[a]	
	Cr	1:1		[a]	
	Mn	1:1		[a]	
	Fe	1:1	40.520	40.211	0.4
			41.137	40.947	
	Co	1:1		[a]	

[a] No signal.

TABLE 2. Crystal parameter of the clathrates M(AcAc)$_3$/*trans*-CHCl=CHCl

M	Space group	Host/guest ratio	D (g/cm^3)		a (Å)	b (Å)	c (Å)	Z	V (Å^3)	Reference
			calc.	meas.						
Al	*Pbca*	1:1	1.33	1.32	7.856(2)	20.212(2)	26.511(13)	8	4210(1)	a
Mn^b	*Pbca*	1:1	1.40	1.37	7.863(2)	20.586(6)	26.376(17)	8	4270(3)	a
Co^b	*Pbca*	1:1	1.45	1.43	7.809(2)	20.256(5)	26.269(4)	8	4155(2)	a
Ga	*Pbca*	1:1	1.45	1.43	7.859(3)	20.422(7)	26.485(10)	8	4251(3)	a
V^b	*P*2$_1$*ca*	1:1	1.38	1.37	7.837(6)	10.203(5)	26.714(9)	4	2136(2)	a
Cr	*P*2$_1$*ca*	1:1	1.41	1.39	7.822(6)	10.211(6)	26.413(17)	4	2110(2)	a
Fe	*P*2$_1$*ca*	1:1	1.40	1.37	7.844(2)	10.244(2)	26.550(5)	4	2134(1)	10

[a] This work. [b] Only cell parameters and space group have been determined.

summary of intensity measurements and structure refinement is given in Table 3 and selected geometrical parameters are reported in Table 4.

Results and discussion

Crystallography

When the Al(AcAc)$_3$ and Ga(AcAc)$_3$ complexes are recrystallized from *trans*-CHCl=CHCl solvent, large yellow and white plate solvent-containing crystals are obtained, respectively. The crystals remain stable as long as they are kept in the solvent atmosphere, but they lose the guest molecule and become porous crystals within half an hour when standing in air. The solvent free porous crystals can absorb the solvent molecules again when brought into the solvent atmosphere. The formation of a host–guest inclusion compound was confirmed by a weight loss analysis of the crystals, and the host/guest ratio of 1:1 was thus determined for these compounds and was reproduced from the crystal density measurements.

Figure 1 shows an atom-numbering stereoscopic view of Al(AcAc)$_3$/*trans*-CHCl=CHCl. Selected geometrical parameters of Al(AcAc)$_3$/*trans*-CHCl=CHCl and Ga(AcAc)$_3$/*trans*-CHCl=CHCl, which use the same atomic labels, are reported in Table 4.

Both Al(AcAc)$_3$/*trans*-CHCl=CHCl and Ga(AcAc)$_3$/*trans*-CHCl=CHCl crystallize in the same orthorhombic class, the space group *Pbca*, and give a volume per host molecule (V/Z) of 526 and 531 Å^3, respectively. These values are much bigger than those of their non-clathrated monoclinic complexes, 431 Å^3 for Al(AcAc)$_3$ [7] and 430 Å^3 for Ga(AcAc)$_3$ [8]. It is evident that these clathrate compounds generate a porous type solid lattice containing cavities. The difference of the volume per molecule between the clathrate compounds and non-clathrated complex should be the cavity volume per molecule. Cavity volumes per molecule of 95 and 101 Å^3 are thus obtained for the Al(AcAc)$_3$ and Ga(AcAc)$_3$ clathrate compounds, and they are considered to be big enough to accommodate one *trans*-CHCl=CHCl guest molecule of a molecular volume of 78 Å^3.

The Al(AcAc)$_3$ and Ga(AcAc)$_3$ host moleculc has a similar geometrical structure to that reported for their non-clathrated complex in the monoclinic phase [7, 8]. Consequently, the trigonal twist angle ϕ and the compression ratio s/h [9] of both Al(AcAc)$_3$ and Ga(AcAc)$_3$ show no significant change from the clathrate phase (ϕ=61.0–61.2°, s/h=1.21–1.22) to the non-clathrated phase (ϕ=62–63°, s/h=1.21). These values indicate that the host molecules Al(AcAc)$_3$ and Ga(AcAc)$_3$ in the clathrate compounds have very little trigonal distortion from the regular octahedral geometry (ϕ=60°, s/h=1.22) [9].

TABLE 3. Summary of intensity measurement and structure refinement for $Al(AcAc)_3$/*trans*-CHCl=CHCl and $Ga(AcAc)_3$/*trans*-CHCl=CHCl

	$Al(AcAc)_3$	$Ga(AcAc)_3$
Formula	$AlC_{15}H_{21}O_6 \cdot C_2H_2Cl_2$	$GaC_{15}H_{21}O_6 \cdot C_2H_2Cl_2$
Crystal dimensions (mm)	0.35×0.30×0.25	0.40×0.30×0.30
Molecular mass (g/mol)	421.25	463.99
Color	yellow	white
Temperature (K)	295	295
$F(000)$	1763.2	1908.4
Reflections used in refinement of cell constants	25	19
λ (Å)	0.70930	0.70930
μ (mm^{-1})	0.38	1.57
Scan technique	ω-scan	ω-scan
2θ Range (°)	35.0–45.0	43.0–50.0
$2\theta_{max}$ (°)	44.9	49.9
Least-squares variables	254	254
Independent reflections	2308	3743
Reflections used in refinements	1542$I > 2.5\sigma(I)$	2298$I > 2.5\sigma(I)$
$R = \Sigma\|\|F_o\| - \|F_c\|\|/\Sigma\|F_o\|$	0.057	0.052
$R_w = [\Sigma w(\|F_o\| - \|F_c\|)^2/\Sigma\|F_o\|^2]^{1/2}$	0.062	0.062
$S = [\Sigma w(\|F_o\| - \|F_c\|)^2(m-n)]^{1/2}$	2.44	1.54
Largest feature final difference map (e $Å^{-3}$)	0.330	0.510

Since the host molecule structures are not significantly changed in the clathrate compounds with respect to their non-clathrated complexes, the host molecules should be rigid, and the formation of the cavity is due to the different molecular packing of the host molecules in the unit cells.

Figure 2 shows the stereoscopic view of the unit cell for $Al(AcAc)_3$/*trans*-CHCl=CHCl. Two guest molecules of *trans*-CHCl=CHCl are stacked above each other in channel-type cavities parallel to the *a* axis. It can be seen from Fig. 3 that the channels are open at the extremity so that the guest molecule can easily escape.

The *trans*-CHCl=CHCl guest molecule is statically disordered in the channels and can have two molecular orientations with 45 and 55% occupancies in the $Al(AcAc)_3$ clathrate compound but 40 and 60% occupancies in the $Ga(AcAc)_3$ clathrate compound. These two molecular orientations can be related by a two-fold symmetric axis passing through the two chlorine atoms (Fig. 4). Thus, the disorder effect does not take place for the chlorine atoms but only the C=C linkage, so the guest molecule is only partially disordered. This disorder effect has not been observed for the $Fe(AcAc)_3$/*trans*-CHCl=CHCl clathrate in the space group $P2_1ca$ [10].

Nuclear quadrupole resonance

The NQR spectra of all clathrate compounds were measured at 77 K. The frequencies can be determined when the separation between two lines is much larger than the linewidth. The temperature dependence of the resonance frequencies has been measured in the region 77–200 K only for the compounds which give distinct and strong signals, and extended to 4 K for some of them.

Site symmetry

The ^{35}Cl nucleus ($I = 3/2$) gives only one resonance line in pure NQR. For a molecule of *n* chlorine atoms, *n* or more than *n* lines should be observed when the molecule is placed in a non-symmetric site. However, when the molecule is located in a cavity with a symmetry, some chlorine atoms can be brought into equivalent positions by the symmetry operation, so that the number of resonances will be reduced to a value less than *n*. Therefore, one can determined the site symmetry of the guest molecule from the number and intensity ratio of the NQR signals.

The *trans*-CHCl=CHCl, CH_2ClCH_2Cl and CH_2Cl_2 molecules have two chlorine atoms. These guest molecules in $M(AcAc)_3$ clathrate compounds show two or more than two resonance lines (Table 1), which indicates that they are all in non-symmetric sites. The same result is also obtained for the $CHCl_3$ clathrates, where more than three signals are usually observed.

The CCl_4/$Fe(AcAc)_3$ clathrate gives an example that the guest molecule is located in a three-fold symmetric site because two NQR signals with an intensity ratio of 1:3 have been obtained. The crystallography con-

TABLE 4. Selected bond lengths (Å) and bond angles (°) in $Al(AcAc)_3$/*trans*-CHCl=CHCl and $Ga(AcAc)_3$/*trans*-CHCl=CHCl

	$Al(AcAc)_3$	$Ga(AcAc)_3$
Bond lengths		
M–O(1)	1.889(4)	1.964(4)
M–O(2)	1.887(4)	1.964(4)
O(1)–C(1)	1.267(7)	1.261(7)
O(2)–C(4)	1.268(7)	1.261(7)
C(1)–C(2)	1.510(9)	1.504(8)
C(1)–C(3)	1.387(9)	1.392(9)
C(3)–C(4)	1.399(9)	1.383(9)
C(4)–C(5)	1.509(8)	1.517(9)
Cl(1)–C(16)	1.696(14)	1.667(20)
Cl(1)–C(16′)	1.748(16)	1.754(14)
Cl(2)–C(17)	1.733(14)	1.808(21)
Cl(2)–C(17′)	1.701(16)	1.735(15)
C(16)–C(17)	1.364(19)	1.387(24)
C(16′)–C(17′)	1.254(22)	1.214(20)
Bond angles		
O(1)–M–O(2)	90.99(18)	90.82(16)
O(1)–M–O(4)	178.95(19)	89.28(16)
M–O(1)–C(1)	129.5(4)	127.1(4)
M–O(2)–C(4)	128.5(4)	125.9(4)
O(1)–C(1)–C(2)	116.4(5)	116.4(5)
O(1)–C(1)–C(3)	123.4(6)	125.1(5)
C(2)–C(1)–C(3)	120.1(5)	118.6(5)
C(1)–C(3)–C(4)	123.2(5)	124.2(5)
O(2)–C(4)–C(3)	124.2(5)	126.4(5)
O(2)–C(4)–C(5)	116.6(5)	114.8(5)
C(3)–C(4)–C(5)	119.2(5)	118.8(6)
Cl(1)–C(16)–C(17)	117.3(9)	115.7(14)
Cl(2)–C(17)–C(16)	118.4(10)	114.7(13)
Cl(1)–C(16′)–C(17′)	121.2(12)	123.6(10)
Cl(2)–C(17′)–C(16′)	122.0(13)	120.1(10)

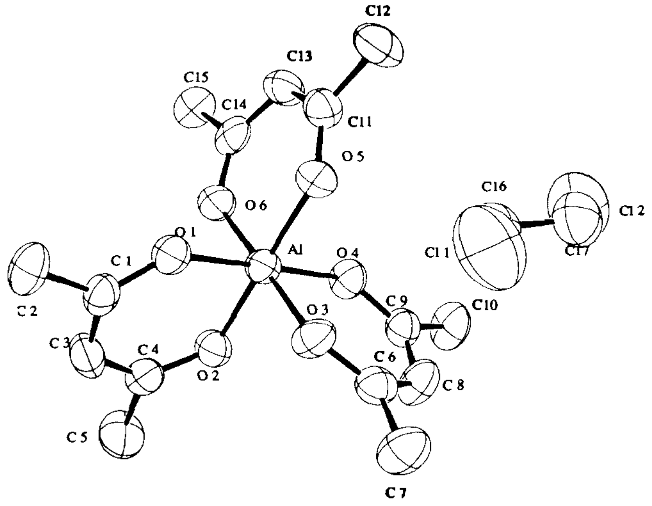

Fig. 1. A labeled ORTEP drawing of $Al(AcAc)_3$/*trans*-CHCl=CHCl with thermal ellipsoids at 50% probability. Hydrogen atoms have been omitted for clarity.

firmed that the clathrate crystallizes in the space group of *R*3, and that the CCl_4 is located in a trigonal cavity [4].

Existence of different crystal phases

The $M(AcAc)_3$/*trans*-CHCl=CHCl clathrate compounds demonstrate the NQR spectra of two groups. Consequently, the clathrates of Al, Ga, Mn and Co have two resonance lines with a large separation (~540 kHz) while the clathrate of V shows two resonance lines with a small separation (~290 kHz); and the clathrates of Cr and Fe have four lines belonging to the two foregoing groups.

These results imply that the guest molecule should be in one of two following situations: the first is that there are two different crystal phases in these compounds. Thus, the clathrates of Al, Ga, Mn and Co crystallize in one phase and the complex of V crystallizes in another, whereas these two phases coexist in the compounds of Fe and Cr; the second is that there are two different molecular sites for the guest molecule in the unit cell of these compounds.

It is unlikely that there are two different molecular sites. Although the intensities of the two lines are equal respectively within the two groups, intensity ratio of the line in these two groups is never close to an integer and is somewhat sample preparation dependent. Consequently it is more reasonable to assume that two crystal phases exist.

The NQR interpretation is confirmed by the crystal structure studies. Indeed, two slightly different crystal structures were observed for the $M(AcAc)_3$/*trans*-CHCl=CHCl clathrates. It can be seen from Table 2 that the clathrates of Al, Mn, Co and Ga have an orthorhombic phase belonging to the space group *Pbca*, whereas the compounds of V, Cr and Fe have also an orthorhombic phase but belonging to the space group $P2_1ba$.

The two crystal phases are very similar and indistinguishable to the eye. The essential difference between the two phases is that the *Pbca* phase is centrosymmetric, but the $P2_1ca$ phase is not; thus the *b* axis and the volume of the unit cell, the number of molecules in the unit cell of the $P2_1ca$ phase are half that of the *Pbca* phase.

The NQR results show that the *Pbca* phase predominates in the Al, Mn, Co and Ga clathrate compounds, while the $P2_1ca$ phase predominates in the V, Cr and Fe clathrates. In fact, the $P2_1ca$ phase has been never observed in the Al, Mn, Co and Ga clathrate compounds and the *Pbca* phase never observed in the V clathrate; the *Pbca* phase occurs in only a small percentage of the crystals of the Fe and Cr clathrate compounds, which is demonstrated by their weaker signals of comparable linewidth.

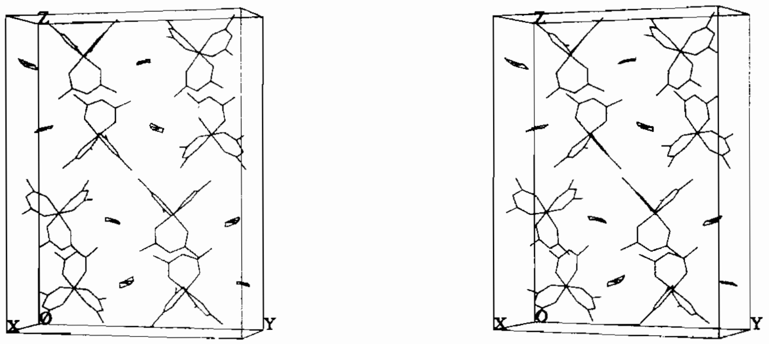

Fig. 2. Stereoscopic view of the unit cell of Al(AcAc)$_3$/*trans*-CHCl=CHCl.

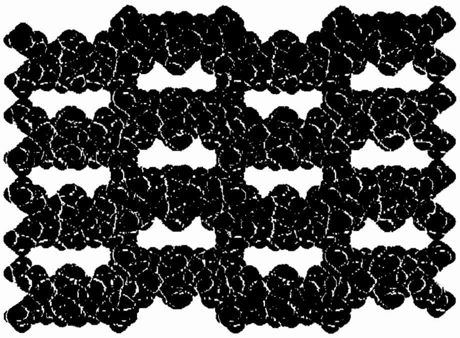

Fig. 3. The CPK representation of four unit cells for the Al(AcAc)$_3$ clathrate down *c* axis (guest molecules are omitted).

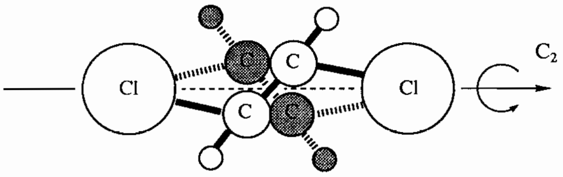

Fig. 4. Two molecular orientations for the *trans*-CHCl=CHCl guest molecule in the cavity.

Although the crystal structures of M(AcAc)$_3$/CH$_2$ClCH$_2$Cl (M=Cr, Mn and Fe) are unknown, two possible crystal phases may be assumed to be present in these clathrate compounds from the NQR results. Thus, two crystal phases can coexist in the Mn clathrate complex, but only one of them predominates in the Cr and Fe clathrate compounds.

The CH$_2$Cl$_2$ and CHCl$_3$ clathrate compounds have the host/guest ratio of 1:2. The multiple lines cannot distinguish whether multiple guest molecule sites or different crystal phases are present in these clathrate compounds. We will undertake crystallographic measurements in an attempt to check this point for the CH$_2$Cl$_2$ and CHCl$_3$ clathrate compounds.

Host–guest interaction

When the guest molecules are placed in a host cavity, the electric field gradient is affected by the electronic distribution of the host molecules. The NQR frequency shift of guest molecules from the clathrate phase to the isolated molecule gives an insight into the host-guest interaction. The relative NQR frequency shifts, $|\Delta\nu_Q|/\nu_Q^{iso}$, are shown in Table 1. $\Delta\nu_Q=\nu_Q-\nu_Q^{iso}$, where ν_Q and ν_Q^{iso} are the average frequencies of the guest molecule in the clathrate and in the isolated molecule.

The shifts of the average frequency are not more than 0.4% for the CH$_2$ClCH$_2$Cl and CCl$_4$ clathrates and indicative of weak intermolecular van der Waals forces, but they are as high as 1.6, 2.5 and 3.0% for the *trans*-CHCl=CHCl, CH$_2$Cl$_2$ and CHCl$_3$ clathrates, respectively, which implies a slightly stronger host–guest interaction through van der Waals forces.

For a given guest molecule, a change of the central metal atom in the host molecule causes only a minor change in the average frequency. This means that the electric field gradient of the guest molecule is very little affected by a variation in the electronic configuration of the metal atom in the host molecules.

Molecular disorder and molecular motions

It can be seen from Table 1 that several guest molecules have no NQR signal in spite of the formation of the clathrates. The absence of signals may be a disorder effect.

The disorder effect is produced by the presence of a large number of different molecular orientations in the crystal. Thus, the resonant nuclei have slightly different chemical environments, and the resonance lines spread over a large region of frequency. The signals become thus too broad and weak to be detected. This conclusion can be confirmed by X-ray analysis, because the host molecules are usually ordered in the crystals, and the guest molecules may be seen disordered.

Dynamical disorder, or molecular motion can also cause the disappearance of the NQR signals. Only rotation and libration play an important role to the

TABLE 5. Calculated parameters for the clathrates M(AcAc)$_3$/*trans*-CHCl=CHCl

M	*Pbca*							*P*2$_1$*ca*						
	ν_{01} (MHz)	ν_{02} (MHz)	f_{t1}^0 (cm^{-1})	f_{t2}^0 (cm^{-1})	g_1 (10^3 K^{-1})	g_2 (10^3 K^{-1})	V_c (Å^3)	ν_{01} (MHz)	ν_{02} (MHz)	f_{t1}^0 (cm^{-1})	f_{t2}^0 (cm^{-1})	g_1 (10^3 K^{-1})	g_2 (10^3 K^{-1})	V_c (Å^3)
Al	34.850	35.399	78.7	81.4	−0.67	−1.11	95	^{a}	^{a}	^{a}	^{a}	^{a}	^{a}	
Ga	34.843	35.395	76.6	76.0	−0.59	−0.84	101	^{a}	^{a}	^{a}	^{a}	^{a}	^{a}	
V	^{a}	^{a}	^{a}	^{a}	^{a}	^{a}		35.007	35.373	62.1	55.0	−0.59	−0.38	101
Cr	^{b}	^{b}	^{b}	^{b}	^{b}	^{b}		35.048	35.274	62.3	60.9	−0.64	−0.75	99
Mn	34.827	35.399	92.8	74.4	−2.04	−0.97	104	^{a}	^{a}	^{a}	^{a}	^{a}	^{a}	
Fe	34.827	35.444	88.8	83.3	−1.51	−2.02		35.067	35.390	64.7	55.5	−0.91	−0.32	98
Co	34.790	35.329	88.7	73.5	−1.20	−0.51	101	^{a}	^{a}	^{a}	^{a}	^{a}	^{a}	

[a] Unobserved. [b] Unsufficient data to compute.

temperature dependence of the NQR frequencies [4]. Thus, rapid and random reorientation makes the average value of the field-gradient tensor zero and the quadrupole relaxation time too short for lines to be detected.

An analytical equation of the Bayer–Kushida [11, 12] form was developed and used to fit the results of the temperature dependence of NQR frequencies and to evaluate quantitatively librational frequencies

$$\nu_Q(T) = \nu_0\left\{1 - \frac{3h}{8\pi^2}\frac{1}{I_t f_t^0}\frac{1}{\exp(hf_t/kT)-1}\right\} \tag{1}$$

where

$$f_t = f_t^0(1 - g_t T) \tag{2}$$

and

$$\frac{1}{I_t} = \sum \frac{1}{I_i} \tag{3}$$

I_t and I_i are the reduced moment of inertia and the moment of inertia of ith normal vibration, respectively; f_t and f_t^0 are thc cffective torsional frequencies above and at 0 K, which include all harmonic or quasi-harmonic vibrations of the molecules, and gives an averaged frequency; g_t is a factor which includes the temperature dependence and anharmonicity of the effective torsional frequency.

The advantage of using this equation is that the function contains only three unknown parameter, ν_0, f_t^0 and g, which can be easily computed. These parameters are important and sufficient to describe the temperature dependence of the NQR frequencies [13], and predict the NQR frequencies at temperatures far from their measurement temperatures.

I_t is obtained from molecular geometrical structure, so ν_0, f_t^0 and g_t parameters can be calculated using eqn. (1) by the non-linear least-squares minimization (NLSM) method [14]. These parameters are calculated and listed in Table 5 for the clathrate compounds M(AcAc)$_3$/*trans*-CHCl=CHCl, and their fitting curves shown in Figs. 5 and 6.

Table 5 shows that the effective libration frequencies, f_t^0, are obtained in the region 73–93 cm^{-1} for the two lines of the clathrates in the *Pbca* phase but 55–65 cm^{-1} for the two lines in the *P*2$_1$*ca* phase. This result indicates that the libration movement is more significant for the guest molecule in the *P*2$_1$*ca* phase, which can also be seen from Figs. 5 and 6 where the resonance frequencies of the clathrates in the *P*2$_1$*ca* phase decrease more quickly in the high temperature region than they do in the *Pbca* phase.

However, the cavity volumes, which are calculated by subtracting the volume per molecule of the clathrate from that of the non-clathrated phase, are nearly the same, i.e. about 100 Å^3, so that the libration movement

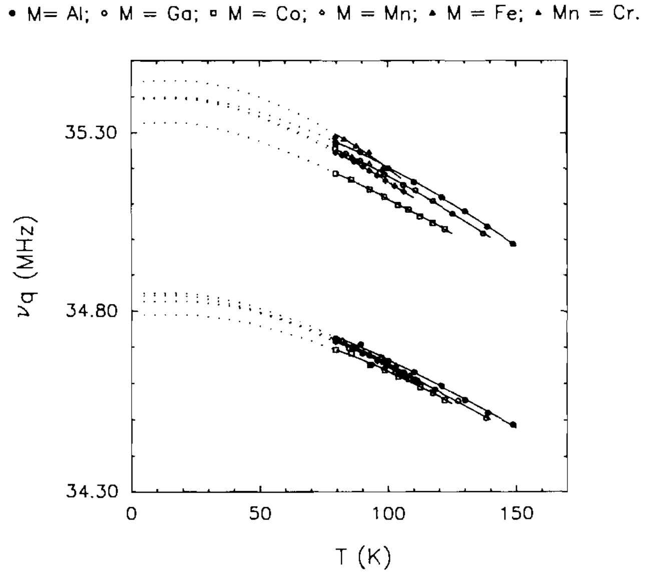

Fig. 5. Temperature dependence of the NQR frequencies of the $M(AcAc)_3$/*trans*-CHCl=CHCl clathrate compounds in the *Pbca* phase.

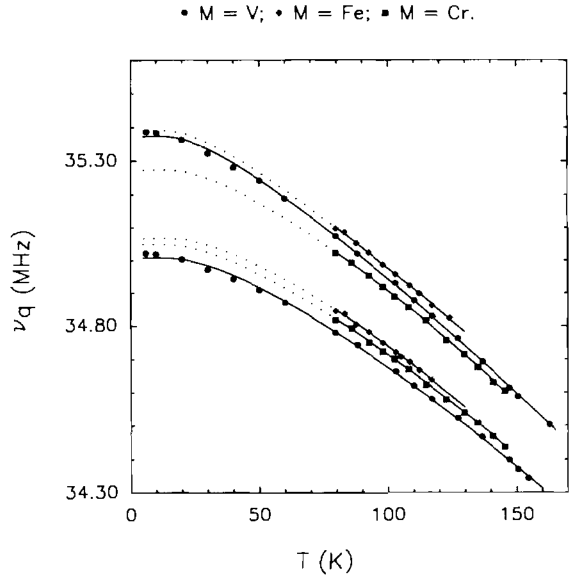

Fig. 6. Temperature dependence of the NQR frequencies of the $M(AcAc)_3$/*trans*-CHCl=CHCl clathrate compounds in the $P2_1ca$ phase.

depends not only on the cavity size but also on the cavity shape.

Supplementary material

Detailed information concerning the crystal structures is available from the authors on request.

Acknowledgements

We thank Dr Hynes for the crystallographic measurements. The National Sciences and Engineering Research Council of Canada and the Swiss National Research Fund support this work.

References

1 D. L. Kepert, in S. G. Wilkinson, R. D. Gillard and J. A. McCleverty (eds.), *Comprehensive Coordination Chemistry,* Vol. 1, Pergamon, Oxford, 1987, pp. 49–68.
2 J. P. Fackler, Jr. and A. Avdeef, *Inorg. Chem., 13* (1974) 1864.
3 J. F. Steinbach and J. H. Burns, *J. Am. Chem. Soc., 80* (1958) 1839.
4 L. Pang, E. A. C. Lucken and G. Bernardinelli, *J. Am. Chem. Soc., 112* (1990) 8754.
5 E. J. Gabe, Y. LePage, J.-P. Charland, F. I. Lee and P. S. White, *J. Appl. Crystallogr., 22* (1989) 384.
6 *International Tables for X-ray Crystallography,* Vol. IV, Kynoch, Birmingham, UK, 1974.
7 P. K. Hon and C. E. Pfluger, *J. Coord. Chem., 3* (1973) 67.
8 K. Dymock and G. J. Palenik, *Acta Crystallogr., Sect. B, 30* (1974) 1364.
9 E. I. Stiefel and G. F. Brown, *Inorg. Chem., 11* (1972) 434.
10 L. Pang, R. C. Hynes and M. A. Whitehead, *Acta Crystallogr., Sect. C, 48* (1992) 1594.
11 H. Bayer, *Z. Phys., 130* (1951) 227.
12 T. Kushida, *J. Sci. Hiroshima Univ. A, 19* (1955) 327.
13 L. Pang, M. A. Whitehead, E. A. C. Lucken and G. Bernardinelli, *J. Chem. Soc., Perkin Trans. II,* (1992) to be published.
14 W. H. Press, B. P. Flannery, S. A. Teukolsky and W. T. Vetterling, *Numerical Recipes,* Cambridge University Press, Cambridge, 1986.